Silicon-carbon fullerenelike nanostructures: An *ab initio* study on the stability of $Si_{60}C_{2n}$ ($n=1, 2$) clusters

A. Srinivasan, M. N. Huda,* and A. K. Ray†
P. O. Box 19059, Department of Physics, The University of Texas at Arlington, Arlington, Texas 76019, USA
(Received 9 July 2005; published 23 December 2005)

Fullerenelike nanostructures of silicon with two and four carbon atoms substituted on the surface of Si_{60} cages, as well as inside the cage at various symmetry orientations, have been studied within the generalized-gradient approximation to density-functional theory. Full geometry optimizations have been performed without any symmetry constraints using the GAUSSIAN 03 suite of programs and the Los Alamos National Laboratory 2 double-ζ basis set. For the silicon atom, the Hay-Wadt pseudopotential with the associated basis set are used for the core electrons and the valence electrons, respectively. For the carbon atom, the Dunning-Huzinaga double-ζ basis set is employed. Electronic and geometric properties of the nanostructures are presented and discussed in detail. It was found that optimized silicon-carbon fullerenelike cages have increased stability compared to the bare Si_{60} cage and the stability depends on the number and orientation of carbon atoms, as well as on the nature of bonding between silicon and carbon atoms.

DOI: 10.1103/PhysRevA.72.063201 PACS number(s): 36.40.Cg, 73.22.−f

I. INTRODUCTION

Experimental and theoretical studies of atomic and molecular clusters continue to be a very active field of research [1–9]. Cagelike compact clusters are particularly important as they can be used as building blocks of more stable materials and the hollow space inside the cage can be doped with different suitable atoms leading to atomically engineered nanostructures with specific scientific and technological applications. For example, well-controlled nanostructures with varying gaps between highest occupied and lowest unoccupied molecular orbitals (HOMO-LUMO gaps) and desired conduction properties can be achieved by controlled the doping of atoms in C_{60} [10]. The spin property of the doped atom inside the cage can be used as the smallest memory device for quantum computers. For example, a tungsten atom in a Si_{12} hexagonal cage is quantum-mechanically isolated from outside so that it can preserve its spin state [11].

Silicon is one of the most extensively used semiconductors in the industry and silicon clusters, preferring sp^3 hybridization, have been studied in detail. *Ab initio* Hartree-Fock-based and density-functional theories (DFT) [12–15] have been used to predict the ground-state structures of bare silicon clusters. Some of these structures are controversial and there are not enough experimental studies for confirmation of the ground-state structures [16]. The discovery of the magically stable C_{60} fullerene cage have prompted scientists to study silicon cagelike fullerene structures, as they can be used as building blocks for fabricating various nanostructures in electronic devices. However, though silicon and carbon belong to the same group of the periodic table, they exhibit different properties due to differences in their nature of bonding. Carbon clusters (C_n) preferring sp^2 hybridization have been found to exist in fullerenelike structures for n as small as 20 [17,18], whereas for silicon clusters (Si_n) these structures are unstable. Studies on the Si_{60} fullerene cage have yielded a distorted cage structure and the Si_{60} fullerene cage is not as stable as C_{60} [19]. Replacing carbon atoms in the C_{60} fullerene cage by silicon atoms has yielded a distorted icosahedral structure [20].

Stabilization of the silicon fullerenelike cage structure with dopant atoms inside has been a major field of study in the last few years. The major goal is twofold: first is to design silicon-based nanostructures with potential applications like carbon fullerenes; and second is to study *possible* magnetic properties of these structures. The second property might be particularly important in memory devices though it has been noted that silicon cages can almost quench the magnetic moments of transition-metal atoms inserted in them [21]. Recent studies have shown that highly stable small silicon cage clusters are possible if transition-metal atoms are encapsulated in the Si cages and in particular, the Si_{20} fullerene by thorium encapsulation [11,22,23]. Bigger clusters like stable Si_{60} fullerenelike cages are possible by doping magic clusters such as $Al_{12}X$ (X=Si, Ge, Sn, Pb), Ba@Si_{20} and $Au_{12}W$ inside the Si_{60} cage [24,25].

In this respect, the combinations of silicon and carbon atoms in a cluster have generated a significant number of studies on carbon-rich structures in fields ranging from cluster science to astrophysics [26]. Studies have been reported for C_{60} inside a Si_{60} fullerenelike cage which yielded a highly distorted structure [24]. Silicon carbide cluster studies have been mostly focused on carbon-rich cage-type clusters and, to the best of our knowledge, silicon-rich cage-type silicon carbide clusters have not been investigated *in detail* so far. We have shown previously using Hartree-Fock-based second-order Moller-Plesset perturbation theory calculations that carbon dimers trapped in medium-sized silicon clusters (Si_n, n=8–14) produces structures comparable in stability to the transition-metal-containing silicon cage clusters [27]. We have also recently reported, using gradient-corrected density-

*Present address: Physics Department, University of Texas at Austin, Austin, Texas 78712.
†Email address: akr@uta.edu

TABLE I. Binding energy per atom (BE) HOMO-LUMO gap; VEA, VIP (all in eV), dipole moment (D), average Si-C bond length (Å), and C-C bond length (Å) for optimized $Si_{58}C_2$ fullerenelike nanostructures.

Structure	State	BE per atom (eV)	HOMO-LUMO gap (eV)	VEA (eV)	VIP (eV)	Dipole moment (D)	Average Si-C bond length (Å)	C-C bond length (Å)
Maindiag	^1A	3.721	0.733	3.637	6.414	0.00	1.85	
Penta-hexa	^1A	3.715	0.687	3.683	6.419	0.83	1.87	1.48
Hexa-hexa	^1A	3.712	0.652	3.646	6.364	0.89	1.91	1.44

functional theory, a class of highly symmetric and stable silicon carbide fullerenelike cage nanostructures with carbon atoms inside the Si_{20} cage [28]. As a continuation of our previous work, we are reporting here our first attempt at stabilizing the Si_{60} cage by adding carbon atoms inside it ($Si_{60}C_2, Si_{60}C_4$) as well as by substitution of silicon atoms by carbon atoms on the surface of the cage ($Si_{58}C_2, Si_{56}C_4$) at different possible orientations. The theoretical formalism of generalized-gradient approximation (GGA) to density-functional theory has been used with the Perdew-Wang (1991) exchange-correlation functional [29]. Full geometry optimizations of the cages has been performed without any symmetry constraints with the Los Alamos National Laboratory 2 double -ζ (LANL2DZ) basis set [30] and GAUSSIAN 03 suite of programs [31]. In this set, for the silicon atom, the Hay-Wadt pseudopotential with the associated basis set is used for the core electrons and the valence electrons. For the carbon atom, the Dunning-Huzinaga double-ζ basis set is employed. All computations have been performed at the supercomputing facilities at the University of Texas at Arlington.

II. RESULTS AND DISCUSSIONS

As is known, the Si_{60} fullerenelike cage has 12 pentagons and 20 hexagons. In the first step, silicon atoms on the surface of the cage were replaced by two and four carbon atoms at various symmetry orientations. In the second step, two and four carbon atoms were put inside the Si_{60} cage at various possible orientations with the carbon atoms parallel and perpendicular to the pentagonal and hexagonal faces. In the third step, as a test of the SiC bond strength, we also put the carbon dimers and tetramers close to the surface, with the same surface orientation, at an initial optimized SiC dimer bond length of 1.77 Å and optimized the structures. For the C_4 ground-state structure, theoretical and experimental studies have reported that there are two structures almost degenerate in energy, one being a rhombus singlet D_{2h} and the other being a triplet linear-chain structure [32]. For this reason, carbon tetramers in a rhombus, a linear chain (as separated dimers), and also in a trigonal planar arrangement optimized at the GGA DFT level of theory have been added inside the cage at various orientations.

In the results to follow, we report the electronic states, binding energy (BE) per atom, HOMO-LUMO gaps, vertical ionization potentials (VIPs), vertical electron affinities (VEAs), and total dipole moments of the stable fullerenelike $Si_{58}C_2, Si_{60}C_2, Si_{56}C_4$, and $Si_{60}C_4$ optimized structures with their corresponding average Si-C and C-C bond lengths. Binding energies per atom of the clusters are calculated as the relative energies of these clusters in the separated-atom limit, with the atoms in their respective ground states. The VIP and VEA are calculated as the difference in the total energies between the neutral clusters and the corresponding positively and negatively charged clusters at the neutral optimized geometries. Harmonic frequencies were also calculated to make sure that the cage structures obtained were not the local minima. Bonding between the atoms, especially Si-C and C-C, for all the stable structures was analyzed using the NBO (natural bonding orbital) program and NBO VIEW [33].

For the set of optimized $Si_{58}C_2$ fullerenelike nanostructures the results are reported in Table I where the column headed "Structures" refers to the positions of the carbon atoms substituting for silicon atoms on the surface of the Si_{60} cage. The optimized geometries of all three structures in Table I are reported in Fig. 1. The structure Maindiag [Fig. 1(a)] has two carbon atoms at diagonally opposite ends of the cage. The structure Penta-hexa [Fig. 1(b)] has two carbon atoms along the common side of a pentagon and a hexagon. The structure Hexa-hexa [Fig. 1(c)] has two carbon atoms along the common side of two hexagons. The first structure Maindiag has the highest BE per atom of 3.721 eV in this set. Its HOMO-LUMO gap of 0.733 eV is also the highest. The total dipole moment of this structure is zero, indicating a highly symmetric charge distribution and strong covalent bonding nature contributing to its increased stability. The average Si-C bond length for this structure is 1.85 Å, which is the smallest in this group, indicating stronger Si-C interaction. There is no C-C bonding in this structure. The Penta-hexa structure has the highest VIP and VEA in this group, but the BE per atom and the HOMO-LUMO gap are slightly lower than for the Maindiag structure. The average Si-C bond length for this structure is slightly higher compared to the Maindiag structure. The total dipole moment for this structure is 0.83 D. The last structure Hexa-hexa has the lowest BE per atom of 3.712 eV and the HOMO-LUMO gap is also the lowest in this set. The C-C bond length for this structure is 1.44 Å, indicating stronger C-C interaction. However, the average Si-C bond length is 1.91 Å, indicating the weakest Si-C interaction for this set. From NBO analysis, the numbers of Si-C bonds in these three structures are found to be eight, six and four respectively, which clearly follow the trend of stability. The vibrational frequencies for the most stable Maindiag structure in this set are listed in supplementary material as Table V [34].

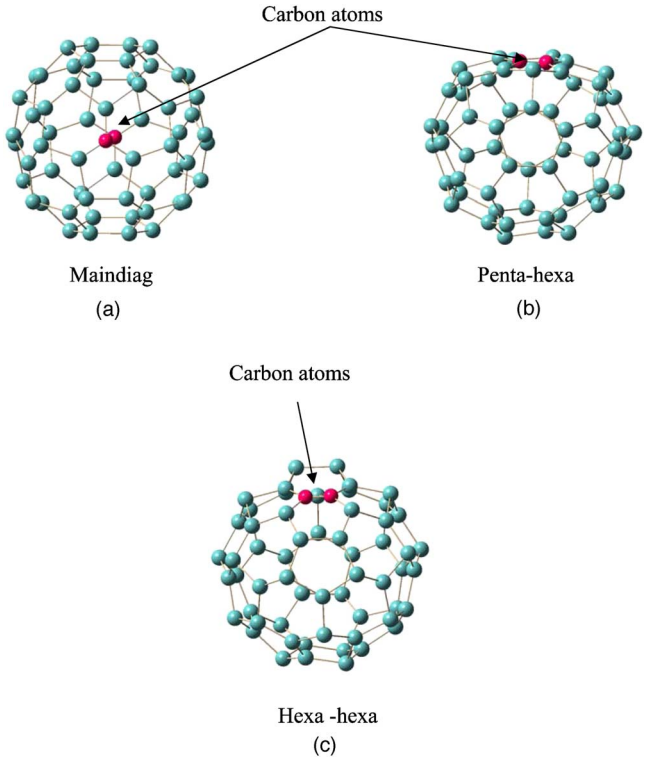

FIG. 1. (Color online) Optimized structures of $Si_{58}C_2$ silicon-carbon fullerene like nanostructures (carbon atoms are denoted by dark pink).

The second set of optimized structures, $Si_{60}C_2$ with carbon atoms inside the Si_{60} cage, are listed in Table II and the corresponding geometries are presented in Fig. 2. Here also the column under the structures represents the orientations of the carbon atoms inside the Si_{60} cage. The Penta-hexa structure [Fig. 2(a)] has the carbon dimer parallel to the common side of a pentagon and a hexagon at the Si-C bond length. The Heper structure [Fig. 2(b)] has the carbon dimer closer to the surface in a plane perpendicular to the hexagonal face of the cage. The Maindiag structure [Fig. 2(c)] has two carbon atoms along the two ends of the perpendicular diagonal at Si-C bond length distance. The Hexa-hexa structure [Fig. 2(d)] has the carbon dimer parallel to the common side of two hexagons at the Si-C bond length distance. The Peper structure [Fig. 2(e)] has the carbon dimer placed closer to the surface in a plane perpendicular to the pentagonal face of the cage. The Hepar structure [Fig. 2(f)] has the carbon dimer closer to the surface in a plane parallel to the hexagonal face of the cage. The structure Pepar [Fig. 2(g)] has the carbon dimer placed closer to the surface in a plane parallel to the pentagonal face of the cage.

The Penta-hexa structure in this set has the highest BE per atom of 3.700 eV. The total dipole moment for this structure is 2.08 D. NBO analysis of this structure yielded four Si-C σ bonds and one C-C double bond. For the next six structures in Table II, the difference in binding energies per atom is at the meV level, the maximum difference being 7 meV. A common feature in these six structures is that all have a C-C triple bond, except Maindiag where there is no C-C bond. It is interesting to note that in general, VEAs for $Si_{60}C_2$ structures are higher, whereas the VIPs and HOMO-LUMO gaps are lower than those of the $Si_{58}C_2$ structures. This indicates relatively higher chemically reactive characteristics for the $Si_{60}C_2$ structures, particularly for the Maindiag structure, which has the highest VEA, the lowest VIP, and the smallest HOMO-LUMO gap. From Fig. 2(c) we note that the two loosely bound silicon atoms may be responsible for these characteristics. Removal of those two silicon atoms makes this structure similar to the $Si_{58}C_2$ Maindiag structure, which is highly stable and relatively less reactive. The Hepar structure has the highest HOMO-LUMO gap and the Hexa-hexa structure has the highest VIP in this set. The vibrational frequencies of the most stable Penta-hexa structure in this set are listed in supplementary material as Table VI [34].

The third set of optimized structures are $Si_{56}C_4$ cages, which have four carbon atoms substituting for the silicon atoms on the surface of the Si_{60} cage. These are reported in Table III and their corresponding geometries are presented in Fig. 3. The structure Hex [Fig. 3(a)] has four carbon atoms at opposite sides of the hexagon. This has the highest BE per atom of 3.819 eV in this set. The total dipole moment of this structure is 1.41 D. NBO analysis of this structure yielded ten Si-C bonds (eight σ bonds, two π bonds), two C-C σ bonds, and one C-C π bond. NBO σ and π bonds between C-C and Si-C for this Hex structure are shown in Fig. 6 below. The vibrational frequencies for the most stable structure of this

TABLE II. Binding energy per atom (BE), HOMO-LUMO gap, VEA, VIP (all in eV), dipole moment (D), average Si-C bond length (Å), and C-C bond length (Å) for optimized $Si_{60}C_2$ fullerenelike nanostructures.

Structure	State	BE per atom (eV)	HOMO-LUMO gap (eV)	VEA (eV)	VIP (eV)	Dipole Moment (D)	Average Si-C bond length (Å)	C-C bond length (Å)
Penta-hexa	^1A	3.700	0.252	3.959	6.260	2.08	1.95	1.43
Heper	^1A	3.685	0.357	3.888	6.289	3.06	1.91	1.29
Maindiag	^3A	3.684	0.157	4.044	6.197	0.57	1.91	
Hexa-hexa	^1A	3.683	0.389	3.854	6.306	1.67	1.93	1.29
Peper	^1A	3.682	0.441	3.783	6.286	2.78	1.91	1.28
Hepar	^1A	3.679	0.496	3.678	6.223	2.16	1.87	1.33
Pepar	^1A	3.678	0.335	3.890	6.273	1.99	1.89	1.29

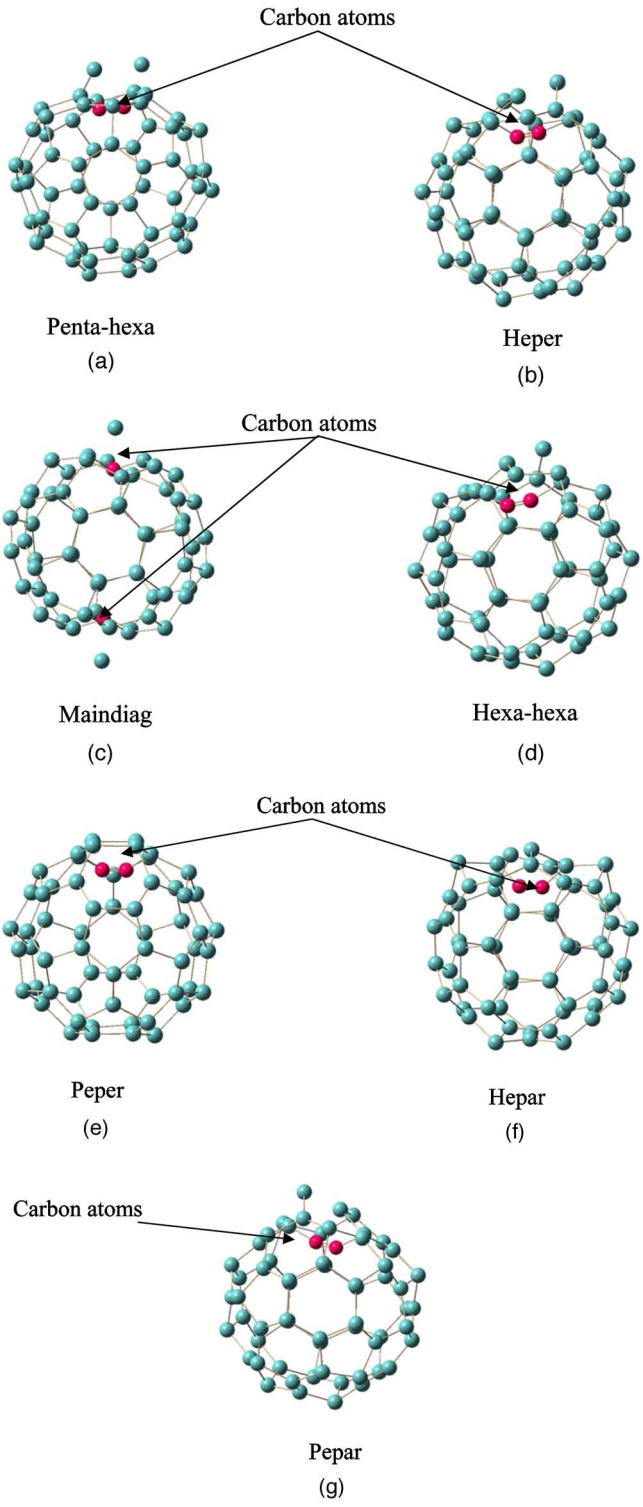

FIG. 2. (Color online) Optimized structures of $Si_{60}C_2$ silicon-carbon fullerene like nanostructures (carbon atoms are denoted by dark pink).

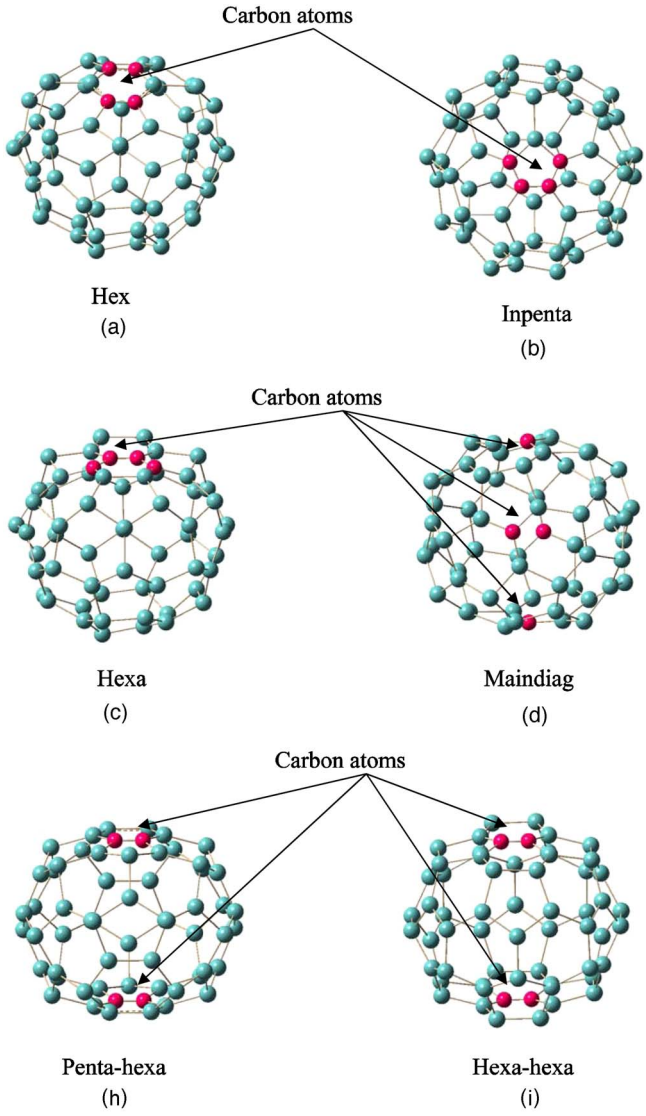

FIG. 3. (Color online) Optimized structures of $Si_{56}C_4$ silicon-carbon fullerene like nanostructures (carbon atoms are denoted by dark pink).

set are listed in supplementary material as Table VII [34]. The structure Inpenta [Fig. 3(b)], which has four carbon atoms at four corners of a pentagon, has almost the same stability as the Hex structure. It has BE per atom of 3.817 eV, 0.002 eV less than the hex structure. The dipole moment of this structure is 0.52 D indicating a slightly less ionic contribution to mixed ionic-covalent bonding. NBO analysis of this structure yielded eight Si-C bonds with six σ bonds and two π bonds, three C-C σ bonds, and one C-C π bond. The structure Hexa [Fig. 3(c)] has four carbon atoms at four corners of a hexagon adjoining two pentagons. The BE per atom is 0.005 eV less than for the Hex structure. The VIP, VEA, and HOMO-LUMO gap for this structure are higher than for the Hex and Inpenta structures. NBO analysis of this structure yielded six Si-C bonds (all σ bonds), three C-C σ bonds, and two C-C π bonds. The number of Si-C bonds in this structure is lower than in the Hex and Inpenta structures. Here again, from the above three structures it might be suggested that the decreasing number of Si-C bonds lowers the binding energy. However, one exception needs to be mentioned. Though the Maindiag structure [Fig. 3(d)] has 16 Si-C bonds (12 σ bonds and four π bonds), the binding energy per atom is 0.008 eV less than the most stable structure of this set. As the four carbon atoms are situated at the opposite ends of two

TABLE III. Binding energy per atom (BE), HOMO-LUMO gap, VEA, VIP (all in eV), dipole moment (D), average Si-C bond length (Å), and average C-C bond length (Å) for optimized $Si_{56}C_4$ fullerenelike nanostructures.

Structure	State	BE per atom (eV)	HOMO-LUMO Gap (eV)	VEA (eV)	VIP (eV)	Dipole moment (D)	Average Si-C bond length (Å)	Average C-C bond length (Å)
Hex	^1A	3.819	0.616	3.645	6.342	1.41	1.87	1.45
Inpenta	^1A	3.817	0.501	3.646	6.244	0.52	1.85	1.48
Hexa	^1A	3.814	0.665	3.655	6.392	1.36	1.88	1.47
Maindiag	^1A	3.811	0.645	3.654	6.369	0.00	1.85	
Tetra	^1A	3.808	0.576	3.690	6.358	0.95	1.85	1.49
Diag	^1A	3.807	0.456	3.742	6.285	0.67	1.86	1.46
Hexb	^1A	3.807	0.601	3.648	6.327	1.18	1.90	1.47
Penta-hexa	^1A	3.805	0.715	3.681	6.457	0.00	1.87	1.48
Hexa-hexa	^3A	3.791	0.255	4.075	5.893	0.01	1.89	1.45

perpendicular diagonals of this cage, there is no C-C bonding. This indicates that C-C bonding also contributes to the stability; the absence of it might be the reason for Maindiag's lower binding energy. The zero dipole moment of this structure indicates a highly symmetric charge distribution and a strong covalent bonding. The Penta-hexa structure [Fig. 3(h)], which has four carbon atoms along the common side of a pentagon and hexagon at two ends of the cage, has the highest HOMO-LUMO gap and VIP in this set. The Hexa-hexa structure has the lowest BE in this set, 3.791 eV per atom. In this structure the two carbon dimers are along the common side of two hexagons at opposite end of the cage. The total dipole moment for this structure is 0.01 D, indicating a very negligible ionic contribution to predominantly covalent bonding. This structure has the lowest VIP and highest VEA in this set. NBO analysis of this structure yielded eight Si-C bonds (all σ bonds). The number of Si-C bonds in this structure is equal to that in the Inpenta structure and higher

TABLE IV. Binding energy per atom (BE), HOMO-LUMO ga, VEA, VIP (all in eV), dipole moment (D), average Si-C bond length (Å), and average C-C bond length (Å) optimized $Si_{60}C_4$ fullerenelike nanostructures.

Structure	State	BE per atom (eV)	HOMO-LUMO gap (eV)	VEA (eV)	VIP (eV)	Dipole moment (D)	Average Si-C bond length (Å)	Average C-C bond length (Å)
Triangle	^1A	3.787	0.453	3.752	6.262	1.67	1.95	1.47
Hexa	^1A	3.783	0.252	3.982	6.253	2.16	1.92	1.44
Inpenta	^1A	3.781	0.454	3.696	6.242	3.80	1.87	1.46
Triangle-pepar	^3A	3.771	0.177	4.048	6.276	1.03	1.92	1.43
Rho-pepar	^1A	3.768	0.506	3.778	6.316	0.62	1.91	1.49
Tetra	^1A	3.762	0.364	3.836	6.248	1.50	1.90	1.45
Rho-heper	^1A	3.761	0.258	4.036	6.311	0.30	1.96	1.43
Hexb	^1A	3.758	0.457	3.810	6.310	1.79	1.93	1.46
Triangle-heper	^1A	3.756	0.512	3.669	6.245	2.39	1.96	1.44
Triangle-peper	^1A	3.755	0.234	4.024	6.310	2.58	1.95	1.43
Rho-peper	^3A	3.747	0.089	4.096	6.228	0.97	1.99	1.44
Rho-hepar	^3A	3.746	0.139	3.948	6.139	1.14	1.96	1.49
Maindiag	^3A	3.746	0.101	4.058	6.171	0.35	1.91	
Lin-pepar	^1A	3.742	0.128	4.131	6.261	0.00	1.91	1.29
Diag	^1A	3.741	0.398	3.756	6.212	2.16	1.87	1.29
Lin-hepar	^1A	3.735	0.427	3.787	6.238	0.01	1.92	1.29
Hexa-hexa	^1A	3.735	0.372	3.826	6.236	3.52	1.92	1.29
Hex	^1A	3.734	0.217	4.088	6.315	1.31	1.90	1.30
Lin-heper	^1A	3.730	0.555	3.748	6.340	0.47	1.94	1.30
Penta-hexa	^1A	3.729	0.437	3.787	6.243	0.37	1.89	1.29

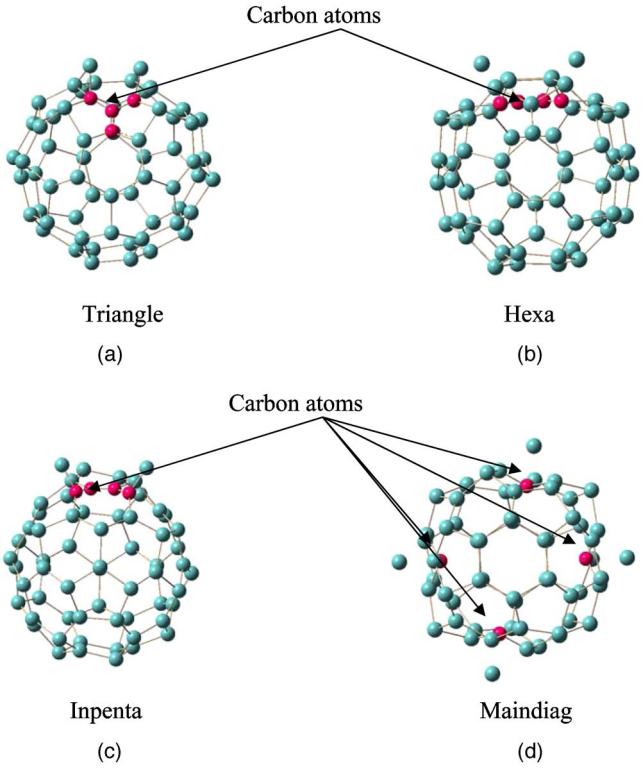

FIG. 4. (Color online) Optimized structures of $Si_{60}C_4$ silicon-carbon fullerene like nanostructures (carbon atoms are denoted by dark pink).

than in the Hexa structure. This also shows that the C-C interactions and their arrangement affect the stability of the cage.

The last set of optimized nanostructures are $Si_{60}C_4$ cages that have four carbon atoms inside the Si_{60} cage. Here also before relaxation all the carbon atoms were placed inside the cage closer to the cage surface and also at Si-C bond length distance. These are reported in Table IV and their corresponding geometries in Fig. 4. From the table it can be seen that some of the structures are degenerate in energy. For the sake of brevity, only a few energetically most favorable structures will be discussed here. There are several structures that are comparable in stability as we increase the number of carbon atoms inside the cage from two to four. For example, binding energies per atom for the first three structures in Table IV are within 6 meV. The structure Triangle [Fig. 4(a)] has four carbon atoms in a trigonal planar arrangement closer to the surface in a plane parallel to a hexagonal face of the cage. This structure has the highest BE per atom of 3.787 eV in the $Si_{60}C_4$ set. The dipole moment is 1.67 D. The vibrational frequencies for this structure were all found to be positive, and these are listed in supplementary material as Table VIII [34]. Next the structure Hexa [Fig. 4(b)] has four carbon atoms parallel to the four corners of a hexagon adjoining two pentagons. The BE per atom is 0.004 eV less than for the Triangle structure. The HOMO-LUMO gap of this structure is lower, but the VEA is higher than for the Triangle structure. The dipole moment of this structure indicates a slight increase in the asymmetric charge distribution compared to the Triangle structure. The average Si-C and C-C bond lengths for this structure are almost the same as before. However the HOMO-LUMO gap is almost half of the Triangle structure's gap. The structure Inpenta [Fig. 4(c)] has four carbon atoms along the four corners of a pentagon. The Si-C and C-C average bond lengths are comparable to the previous two structures. The Inpenta structure's BE per atom is 0.002 eV less than for the Hexa structure. It can be noted from Table IV that the dipole moments of all these three structures are higher than for the previously discussed structures; particularly for Inpenta, which is the highest, 3.80 D. The highly asymmetric structure for these cages is responsible for this increased dipole moment.

A common feature of the above $Si_{60}C_4$ structures is that the carbon atoms pushed a few silicon atoms outside the cage, and as a result those silicon atoms become loosely bound to the cage. This is one of the main reason for the lower binding energy of these set compared to $Si_{56}C_4$ cages. For example, the structure Maindiag [Fig. 4(m)] in this set has no C-C bonding and has a low dipole moment, indicating a strong covalent bonding and a highly symmetric charge distribution, but the BE per atom is 0.041 eV less than for the most stable Triangle structure. Absence of C-C bonding might be one of the reasons for the lower binding energy, but the primary reason is that the four silicon atoms that are pushed out by the carbon atom are loosely bound to the cage. It is interesting to compare this structure with the $Si_{56}C_4$ Maindiag structure. Both the structures are similar, except for the four loosely bound silicon atoms that are removed from the $Si_{60}C_4$ cage, which resulted in 0.065 eV per atom increase in binding energy and caused the structure to become more stable than the most stable structure of the $Si_{60}C_4$ set, the Triangle structure. In addition to this the difference between the binding energy of the $Si_{56}C_4$ Hex structure, highest in that group, and the Maindiag structure is 0.008 eV per atom. This example suggests that the mere presence of the C-C bonding would not significantly increase the binding energy; it is the Si-C interaction that is important. The most stable Triangle structure has eight Si-C bonds, all of which are σ bonds. The next two structures, Hexa and Inpenta, each have six Si-C bonds, which is less than for the Triangle structure. This again might indicate that Si-C interaction is important for stability.

In addition to the above structures, several other possibilities were also tried. It was mentioned above that carbon atoms (two and four) put inside the Si_{60} cage at various orientations closer to the cage surface move closer to the surface and bond with silicon atoms, thereby pushing one or two silicon atoms outside the surface of the fullerenelike cage. The silicon atoms that were pushed out of the $Si_{60}C_4$ and $Si_{60}C_2$ cages were removed and the corresponding structures were reoptimized. The reoptimized structures showed higher stability as expected from the removal of silicon atoms but were barely as stable as $Si_{56}C_4$ and $Si_{58}C_2$ clusters. We also tried to put carbon atoms at the center of the Si_{60} cages, but the structures were not stable. From Tables I–IV, it is clear that there is a general tendency for increase in the binding energy per atom with increase in the number of carbon atoms. In general, all the optimized structures considered here are stable nanostructures with higher binding energies per atom compared to the bare Si_{60} cage, which has a binding

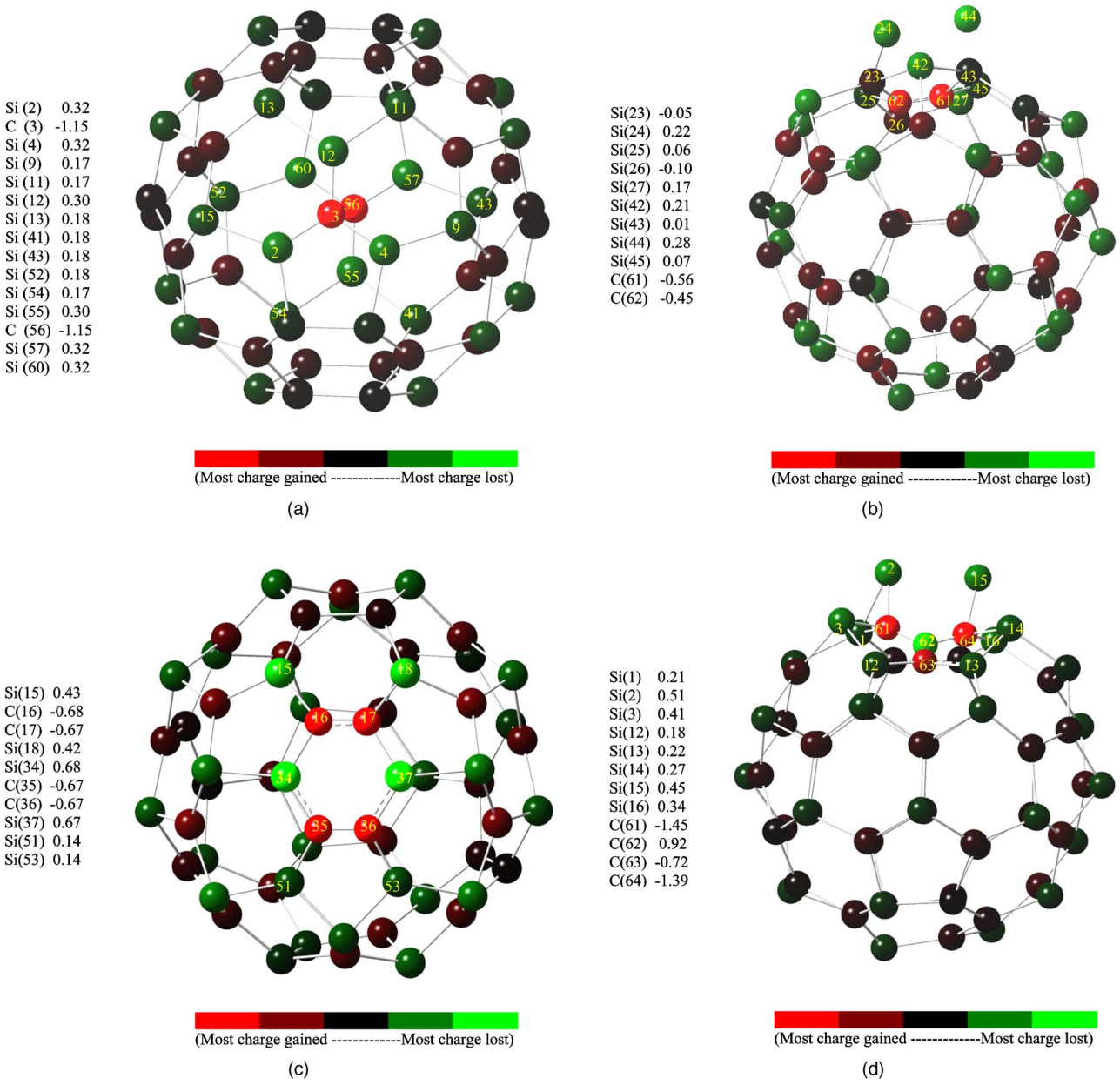

FIG. 5. (Color online) (a) Mulliken charge distribution for the most stable Maindiag ($Si_{58}C_2$) structure. Selected atom labels with their respective electronic charge are shown in the figure. (b) Mulliken charge distribution for the most stable penta-hexa ($Si_{60}C_2$) structure. Selected atom labels with their respective electronic charge are shown in the figure. (c) Mulliken charge distribution for the most stable hex ($Si_{56}C_4$) structure. Selected atom labels with their respective electronic charge are shown in the figure. (d) Mulliken charge distribution for the most stable triangle ($Si_{60}C_4$) structure. Selected atom labels with their respective electronic charge are shown in the figure.

energy per atom of 3.61 eV at the GGA DFT level of theory. Also, the carbon atoms substituting for silicon atoms on the surface of the Si_{60} fullerene cage give higher binding energies than carbon atoms put inside the Si_{60} cage. Thus, the stability of the nanostructures is found to be dependent on the number of carbon atoms and their orientations inside or on the surface of the fullerenelike cage.

As mentioned before, for the most part the carbon-carbon interaction does not contribute significantly to the cage stability. It is the Si-C interaction that is important. For example, from Table I we note that for the most stable structure there is no C-C interaction, while in Table II, the Maindiag ($Si_{60}C_2$), where there is no C-C bonding, is only 0.016 eV/atom less stable than the most stable structure in that group. Similar conclusions can be made for the $Si_{56}C_4$ group (Table III). In fact a part of the C-C interaction sometimes slightly offsets the increased stability of the cages due to the fact that carbon atoms usually acquire some charges and their mutual Coulomb interaction is repulsive. However, for the $Si_{60}C_4$ group (Table IV), the difference between the BE of the most stable structure and that where there is no C-C bond is slightly higher, 0.041 eV/atom, which is approximately 1% of the total binding energy. Considering the fact that inclusion of carbon atoms increased the Si_{60} cage

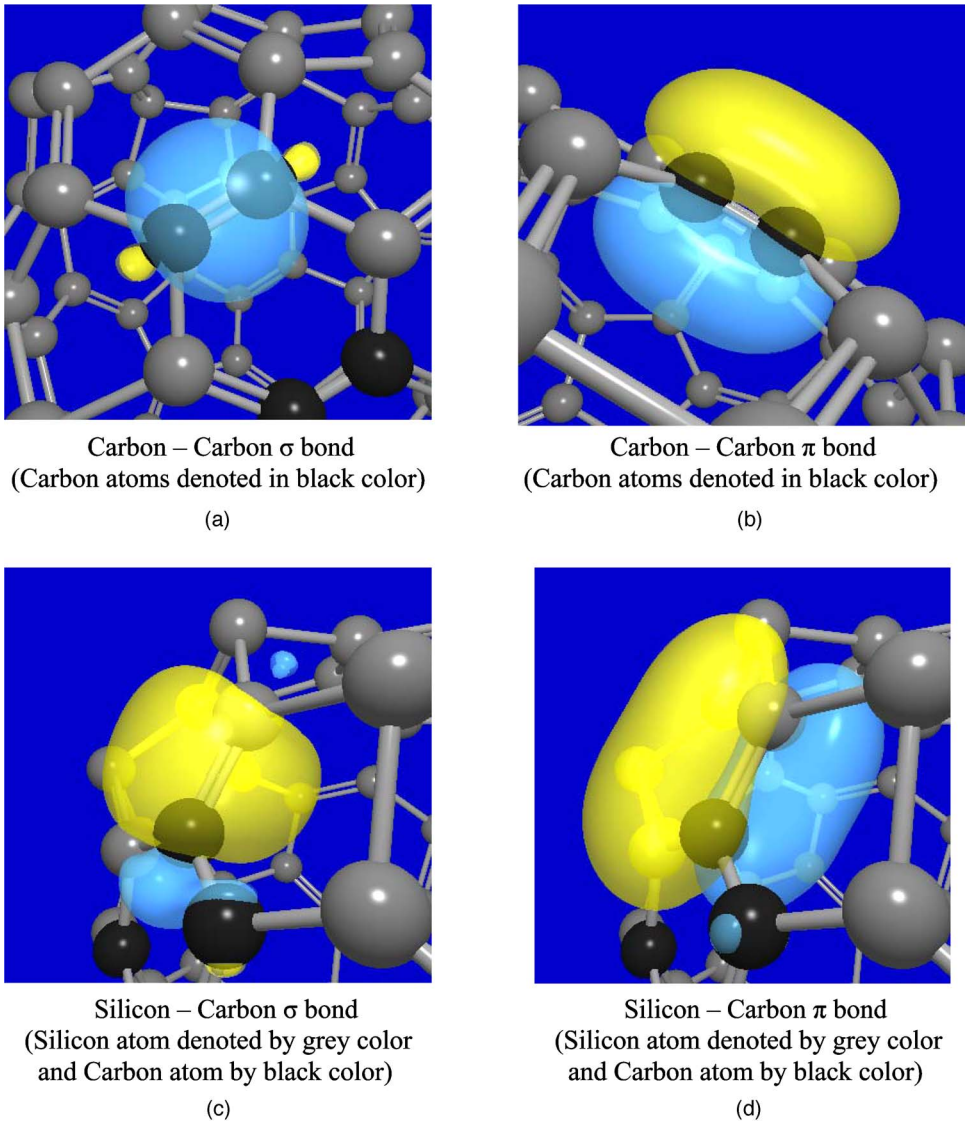

FIG. 6. (Color online) Natural bond orbital (NBO) plots generated using the NBO program and NBO the view for the most stable hex structure ($Si_{56}C_4$). (a) Carbon-carbon σ bond (carbon atoms are denoted by black). (b) Carbon-carbon π bond (carbon atoms are denoted by black). (c) Silicon-carbon σ bond (the silicon atom is denoted by gray and the carbon atom by black). (d) Silicon-carbon π bond (the silicon atom is denoted by gray and the carbon atom by black color).

binding energy by almost 5% for this structure, 1% is a significant contribution. The asymmetric charge distribution on the carbon atoms and the cage is responsible for this [Fig. 5(d)] increase in total binding energy in the Triangle structure. In this structure, the four carbon atoms are arranged in a planar triangular form, where the carbon atom at the center of the triangle is positively charged, and has no bonding with the silicon atoms. So the increased C-C attractive Coulomb interaction is added to the binding energy, and is responsible for the above fact. However, it should be noted that despite this increased attractive C-C interaction, $Si_{60}C_4$ structures are less stable than the $Si_{56}C_4$ Maindiag structure, where C-C interactions do not play any significant role.

In general, Mulliken charge analysis for all the structures clearly indicates that carbon atoms gain charge and silicon atoms lose charge, as expected from their electronegativity. Mulliken charge distribution diagrams for the four most stable structures in each set generated using GAUSSIAN 03 along with the electronic charges for selected groups of atoms are reported in Figs. 5(a)–5(d). All the charges are noted in electronic charge units. In general these structures have mostly covalent and partly ionic bonding between the silicon and carbon atoms. For example, in the $Si_{56}C_4$ Hex structure [Fig. 5(c)], four carbon atoms (labels 16, 17, 35, and 36) along the opposite corners of the hexagon have electronic charges of $-0.68, -0.67, -0.67$, and -0.67, respectively, and they are bonded to six silicon atoms (labels 15, 18, 34, 37, 51, and 53) having electronic charges of 0.43, 0.42, 0.68, 0.67, 0.14, and 0.14, which clearly indicates mixed ionic and covalent bonding, with covalent being more prominent. From Fig. 5(d), we notice an exception in the Mulliken charge distribution for the Triangle structure ($Si_{60}C_4$) as the center carbon atom for a C_4 trigonal planar arrangement inside the cage did lose charge to three other nearby carbon atoms. The carbon atoms labeled 61, 62, 63, and 64 and their Mulliken electronic charges (-1.45, 0.92, -0.72, and -1.39) clearly show positive electronic charge for a carbon atom, indicating an attractive Coulomb interaction between the four carbon atoms. As mentioned earlier, this adds to the cage stability, but may not result in fullerene-type structures because of its ionic nature. The VIPs and the VEAs for all the optimized nanostructures reported in this work are considerably higher, indicating stability. The VIPs and the VEAs do not follow any specific pattern with the number

of carbon atoms in the Si_{60} cage. In general, the Mulliken charge analysis for silicon-carbon fullerenelike nanostructures indicates a more covalent bonding nature, except for the last one, $Si_{60}C_4$, where the ionic contribution also becomes significant.

III. CONCLUSIONS

In conclusion, we have studied a class of stable $Si_{60}C_{2n}$ ($n=1, 2$) fullerenelike nanostructures. These structures have increased stability compared to the bare Si_{60} cage and their stability depends on the number and orientation of carbon atoms, as well as on the coordination of carbon to silicon atoms in the cage. All the ground-state structures we have studied here are in the singlet state, i.e., no magnetic structures have been found. In the case of two carbon atoms on the surface of the Si_{60} cage, mainly covalent bonding contributed to the stability and for other structures a mixture of ionic and covalent bonding contributed to their stability. Except for the most stable $Si_{60}C_4$, C-C interactions do not have significant impact on the stability of the silicon cages; rather, Si-C interactions appear to be more important. In a given group, again except for $Si_{60}C_4$, binding energies do not change significantly due to the particular arrangements of the carbon atoms. However, for $Si_{60}C_4$, the C-C interactions and the C atom orientations have considerable effect. For example, the difference in binding energy between the most stable and least stable isomers of $Si_{60}C_4$ is 1.55%, out of the total increase of 5% due to the insertion of carbon atoms in the Si_{60} cage. These observations, along with the fact that carbon atoms do not stabilize the Si_{60} cage if they are placed at the center of the cage, suggest that as the number of carbon atoms is increased in the cage, the local Si-C interactions are the dominant factor in deciding the stability of the clusters. Hence we may suggest that proper arrangements with more carbon atoms might be needed to have a more stabilized and smoother fullerenelike silicon nanostructure. Further theoretical and experimental studies are needed to understand the hybrid nature of the bonding and the stability of the cages reported in this study.

ACKNOWLEDGMENT

This work is partially supported by the Welch Foundation, Houston, Texas (Grant No. Y-1525).

[1] *Atomic and Molecular Clusters*, edited by E. R. Bernstein (Elsevier, New York, 1990).
[2] *Physics and Chemistry of Finite Systems—From Clusters to Crystals*, edited by P. Jena, S. N. Khanna, and B. K. Rao, Proceedings of the NATO Advanced Research Workshop (Kluwer Academic Publishing, Dordrecht, 1991).
[3] *Clusters of Atoms and Molecules*, edited by H. Haberland (Springer-Verlag, Berlin, 1994).
[4] U. Naher, S. Bjornholm, S. Frauendorf, F. Garcias, and C. Guet, Phys. Rep. **285**, 245 (1997).
[5] S. Sugano and H. Koizumi, *Microcluster Physics* (Springer-Verlag, New York, 1998).
[6] *Theory of Atomic and Molecular Clusters: With a Glimpse at Experiments*, edited by J. Jellinek, R. S. Berry, and J. Jortner (Springer-Verlag, New York, 1999).
[7] S. Bjornholm and J. Borggreen, Philos. Mag. B **79**, 1321 (1999).
[8] P. Jena, S. N. Khanna, and B. K. Rao, *Theory of Atomic and Molecular Clusters* (Springer-Verlag, Berlin, 1999).
[9] Roy L. Johnston and R. L. Johnston, *Atomic and Molecular Clusters* (Routledge Publishing, New York, 2002).
[10] N. E. Frick, M. S. thesis, The University of Texas at Arlington, 2002 (unpublished), and references therein; N. E. Frick, A. S. Hira, and A. K. Ray (unpublished).
[11] H. Hiura, T. Miyazaki, and T. Kanayama, Phys. Rev. Lett. **86**, 1733 (2001); T. Miyazaki, H. Hiura, and T. Kanayama, Phys. Rev. B **66**, 121403(R) (2002).
[12] A. Szabo and N. S. Ostlund, *Modern Quantum Chemistry* (Macmillan, New York, 1982).
[13] W. J. Hehre, P. v. R. Schleyer, and J. A. Pople, *Ab Initio Molecular Orbital Theory* (Wiley, New York, 1982).
[14] R. G. Parr and W. Yang, *Density Functional Theory of Atoms and Molecules* (Oxford University Press, New York, 1989).
[15] L. R. Marim, M. R. Lemes, and A. Dal Pino, Jr., J. Mol. Struct.: THEOCHEM **663**, 159 (2003).
[16] K.-M. Ho, A. A. Shvartsburg, B. Pan, Z.-Y. Lu, C.-Z. Wang, J. G. Wacker, J. L. Fye, and M. F. Jarrold, Nature (London) **392**, 582 (1998).
[17] G. V. Helden, M. T. Hsu, N. Gotts, and M. T. Bowers, J. Phys. Chem. **97**, 8182 (1993).
[18] M. F. Jarrold, Nature (London) **407**, 26 (2000); J. C. Grossman, L. Mitas, and K. Raghavachari, Phys. Rev. Lett. **75**, 3870 (1995).
[19] B.-X. Li, P.-L. Cao, and D.-L. Que, Phys. Rev. B **61**, 1685 (2000); B.-X. Li, P.-L. Cao, B. Song, and Z.-Z. Ye, J. Mol. Struct.: THEOCHEM **620**, 189 (2003); M. C. Piqueras, R. Crespo, E. Orti, and F. Tomas, Chem. Phys. Lett. **213**, 509 (1993); R. Crespo, M. C. Piqueras, and F. Tomas, Synth. Met. **77**, 13 (1996); K. Jug and M. Krack, Chem. Phys. **173**, 439 (1993); F. S. Khan and J. Q. Broughton, Phys. Rev. B **43**, 11754 (1991); Z. Chen, H. Jiao, G. Seifert, A. H. C. Horn, D. Yu, T. Clark, W. Thiel, and P. V. R. Schleyer, J. Comput. Chem. **24**, 948 (2003); M. Menon, and K. R. Subbaswamy, Chem. Phys. Lett. **219**, 219 (1994).
[20] M. Menon, J. Chem. Phys. **114**, 7731 (2001).
[21] S. N. Khanna, B. K. Rao, and P. Jena, Phys. Rev. Lett. **89**, 016803 (2002); W. Zheng, J. M. Nilles, D. Radisic, and K. H. Bowen, J. Chem. Phys. **122**, 071101 (2005).
[22] K. Jackson and B. Nellermoe, Chem. Phys. Lett. **254**, 249 (1996); V. Kumar and Y. Kawazoe, Phys. Rev. Lett. **87**, 045503 (2001); Phys. Rev. B **65**, 073404 (2002); H. Kawamura, V. Kumar, and Y. Kawazoe, *ibid.* **70**, 245433 (2004); C. Xiao, F. Hagelberg, and W. A. Lester, *ibid.* **66**, 075425 (2002).
[23] A. K. Singh, V. Kumar, and Y. Kawazoe, Phys. Rev. B **71**,

115429 (2005).

[24] Q. Sun, Q. Wang, P. Jena, B. K. Rao, and Y. Kawazoe, Phys. Rev. Lett. **90**, 135503 (2003); Q. Sun, Q. Wang, P. Jena, J. Z. Yu, and Y. Kawazoe, Sci. Technol. Adv. Mater. **4**, 361 (2003).

[25] Q. Sun, Q. Wang, Y. Kawazoe, and P. Jena, Eur. Phys. J. D **29**, 231 (2004).

[26] V. D. Gordon, E. S. Nathan, A. J. Apponi, M. C. McCarthy, P. Thaddeus, and P. Botschwina, J. Chem. Phys. **113**, 5311 (2000); J. Cernicharo, C. A. Gottlieb, M. Guelin, P. Thaddeus, and J. M. Vrtilek, Astrophys. J. **341**, L25 (1989); M. Oshishi, N. Kaifu, K. Kawaguchi, A. Murakami, S. Saito, S. Yamamoto, S.-I. Ishikawa, Y. Fujita, Y. Shiratori, and W. M. Irvine, *ibid.* **34**, L83 (1989); S. Hunsicker and R. O. Jones, J. Chem. Phys. **105**, 5048 (1996); S. Osawa, M. Harada, and E. Osawa, Fullerene Sci. Technol. **3**, 225 (1995); M. Pellarin, C. Ray, J. Lerme, J. L. Vialle, M. Broyer, X. Blase, P. Keghelian, P. Melinon, and A. Perez, J. Chem. Phys. **110**, 6927 (1999); C. Ray, M. Pellarin, J. L. Lerme, J. L. Vialle, M. Broyer, X. Blase, P. Keghelian, P. Melinon, and A. Perez, Phys. Rev. Lett. **80**, 5365 (1998); W. Branz, I. M. L. Billas, N. Malinowski, F. Tast, M. Heinebrodt, and T. P. Martin, J. Chem. Phys. **109**, 3425 (1998); P. Pradhan and A. K. Ray, J. Mol. Struct.: THEOCHEM **716**, 109 (2004).

[27] M. N. Huda and A. K. Ray, Phys. Rev. A **69**, 011201(R) (2004).

[28] M. N. Huda and A. K. Ray, Eur. Phys. J. D **31**, 63 (2004).

[29] J. P. Perdew, K. Burke, and Y. Wang, Phys. Rev. B **54**, 16533 (1996); J. P. Perdew, K. Burke, and M. Ernzerhof, Phys. Rev. Lett. **77**, 3865 (1996); J. P. Perdew, J. A. Chevary, S. H. Vosko, K. A. Jackson, M. R. Pederson, D. J. Singh, and C. Fiolhais, Phys. Rev. B **46**, 6671 (1992); J. P. Perdew, J. A. Chevary, S. H. Vosko, K. A. Jackson, M. R. Pederson, D. J. Singh, and C. Fiolhais, Phys. Rev. B **48**, 4978 (1993).

[30] P. J. Hay and W. R. Wadt, J. Chem. Phys. **82**, 284 (1985).

[31] M. J. Frisch *et al.*, Computer code Revision C.02 GAUSSIAN 03, (Gaussian Inc., Pittsburgh, PA, 2003).

[32] A. K. Ray, J. Phys. B **20**, 5233 (1987); L. S. Ott and A. K. Ray, in *Proceedings of the NATO Advanced Workshop and International Symposium on the Physics and Chemistry of Small Clusters*, edited by P. Jena, B. K. Rao, and S. N. Khanna (Plenum, New York, 1987), p. 95; K. Raghavachari and J. S. Binkley, J. Chem. Phys. **87**, 2191 (1987); R. O. Jones, *ibid.* **110**, 5189 (1999); A. V. Orden and R. J. Saykally, Chem. Rev. (Washington, D.C.) **98**, 2313 (1998); C. Zhang, X. Xu, H. Wu, and Q. Zhang, Chem. Phys. Lett. **364**, 213 (2002); W. Chai, N. Shao, X. Shao, and Z. Pan, J. Mol. Struct.: THEOCHEM **678**, 113 (2004); B. R. Eggen, R. L. Johnston, and J. N. Murell, J. Chem. Soc., Faraday Trans. **90**, 3029 (1994).

[33] E. D. Glendening, J, K. Badenhoop, A. E. Reed, J. E. Carpenter, J. A. Bohmann, C. M. Morales, and F. Weinhold, Computer code NBO 5.0 (Theoretical Chemistry Institute, University of Wisconsin Madison, 2001).

[34] See, EPAPS Document No. E-PLRAAN-72-115512 for figures and frequencies not shown in the text. This document can be reached via a direct link in the online article's HTML reference section or via the EPAPS homepage (http://www.aip.org/pubservs/epaps.html).